Carnegie Observatories Astrophysics Series, Vol. 4:
Origin and Evolution of the Elements, 2004
ed. A. McWilliam and M. Rauch (Cambridge: Cambridge Univ. Press)

Chemical Composition of the Intracluster Medium

MICHAEL LOEWENSTEIN
NASA/Goddard Space Flight Center and University of Maryland

Abstract

Clusters of galaxies are massive enough to be considered representative samples of the Universe, and to retain all of the heavy elements synthesized in their constituent stars. Since most of these metals reside in hot plasma, X-ray spectroscopy of clusters provides a unique and fundamental tool for studying chemical evolution. I review the current observational status of X-ray measurements of the chemical composition of the intracluster medium, and its interpretation in the context of the nature and history of star and galaxy formation processes in the Universe. I provide brief historical and cosmological contexts, an overview of results from the mature *ASCA* observatory database, and new results from the *Chandra* and *XMM-Newton* X-ray observatories. I conclude with a summary of important points and promising future directions in this rapidly growing field.

1.1 Introduction

1.1.1 Rich Clusters of Galaxies and their Cosmological Setting

Rich clusters of galaxies, characterized optically as concentrations of hundreds (or even thousands) of galaxies within a region spanning several Mpc, are among the brightest sources of X-rays in the sky, with luminosities of up to several 10^{45} erg s^{-1}. The hot intracluster medium (ICM) filling the space between galaxies has an average particle density $\langle n_{\rm ICM}\rangle \approx 10^{-3}$ cm^{-3} and an electron temperature ranging from 20 to > 100 million K. Interpreted as virial temperatures, these correspond to masses of $\sim (1-20) \times 10^{14}\ M_{\odot}$; rich clusters are believed to be the largest gravitationally bound structures in the Universe. They are also notable for their high fraction (typically $\sim 75\%$) of member galaxies of early-type morphology, as compared to galaxy groups or the field. Within the framework of large-scale structure theory, rich clusters arise from the largest fluctuations in the initial random field of density perturbations, and their demographics are sensitive diagnostics of the cosmological world model and the origin of structure (e.g., Schuecker et al. 2003). Rich galaxy clusters are rare and (including their dark matter content) account for less than 2% of the critical density, $\rho_{\rm crit}$, characterizing a flat Universe.

Embedded in the ICM of rich clusters—where $70\% - 80\%$ of cluster metals reside—lies a uniquely accessible fossil record of heavy element creation. To the extent that the cluster galaxy stars where these metals were synthesized are representative, measurement of ICM chemical abundances provides constraints on nucleosynthesis—and, by extension, the epoch, duration, rate, efficiency, and initial mass function (IMF) of star formation—in the

Table 1.1. *Mass-to-Light Ratios and Mass Fractions*

Parameter	Universe	Clusters
$\langle M_{\rm total}/L_B \rangle$	270	300
$\langle M_{\rm stars}/L_B \rangle$	3.5	4
$\langle M_{\rm gas}/L_B \rangle$	41	35
$f_{\rm baryon}$	0.17	0.13
$f_{\rm stars}$	0.013	0.013
$f_{\rm gas}$	0.15	0.12
stars/gas	1/12	1/9

Universe. From this perspective it is useful to take an inventory of clusters, and compare with the Universe as a whole.

Consideration of recent results from the *Wilkinson Microwave Anisotropy Probe* supports a standard cosmological model wherein, to high precision, the average matter density totals $0.27\rho_{\rm crit}$ in a flat Universe, and baryons amount to $0.044\rho_{\rm crit}$ (Spergel et al. 2003). The estimate of Fukugita, Hogan, & Peebles (1998) of the total density in stars, $\sim 0.0035\rho_{\rm crit}$, is corroborated by recent constraints based on the extragalactic background light (Madau & Pozzetti 2000), and the Two Micron All-Sky Survey and Sloan Digital Sky Survey (Bell et al. 2003). Since critical density corresponds to a mass-to-light ratio (B band) $M/L_B \approx 1000$, the cluster matter inventory compares to the Universe as a whole as indicated in Table 1.1.

Deviations from the typical rich cluster values displayed in Table 1.1 are found for both the total mass-to-light ratio and the baryonic contributions (Ettori & Fabian 1999; Mohr, Mathiesen, & Evrard 1999; Bahcall & Comerford 2002; Girardi et al. 2002; Lin, Mohr, & Stanford 2003)—indicative of differences and uncertainties in assumptions, method of calculation, and in extrapolation to the virial radius, as well as possible cosmic variance. However, it is clear that, at least to first order, observations are consistent with the theoretical expectation (e.g., Evrard 1997) that these largest virialized structures are "fair samples" of the Universe in terms of their mix of stars, gas, and dark matter. (A corollary of this is that bulge populations generally dominate the stellar mass budget in the field, as well as in clusters.) While clusters were the first systems identified with baryon budgets dominated by a reservoir of hot gas (White et al. 1993), this is now believed to apply to the Universe as a whole at past and present epochs (Davé et al. 2001; Finoguenov, Burkert, & Bohringer 2003).

An important *caveat* is that, since rich clusters do represent regions of largest initial overdensity, star formation may initiate at higher redshift, proceed with enhanced efficiency, or be characterized by an IMF skewed toward higher mass stars when compared to more typical regions. If so, there is an opportunity to search for possible variations in star formation with epoch or environment, given a suitable class of objects for comparison.

The intergalactic medium in *groups* of galaxies may comprise one such sample. Groups generally include $\sim 2-50$ member galaxies, emit at X-ray luminosities $< 10^{44}$ erg s^{-1}, and have electron temperatures < 20 million K, corresponding to mass scales up to $\sim 10^{14}$ $M_\odot$ (Mulchaey 2000). Groups present their own unique interpretive challenges. They may not behave as closed boxes and evidently display a spread in their mass inventories, metallicities, and morphological mix of galaxies that reflect the theoretically expected cosmic variance in formation epoch and evolution (Davis, Mulchaey, & Mushotzky 1999; Hwang et al. 1999). However, since extending consideration to the poorest groups encompasses most of the galaxies (and stars) in the Universe, it is crucial to study the chemical composition of the intragroup, as well as the intracluster, medium.

1.1.2 Advantages of X-ray Wavelengths for Abundance Studies

From both scientific and practical perspectives, X-ray spectroscopy is uniquely well suited for studying the chemical composition of the Universe. Most of the metals in the Universe are believed to reside in the intergalactic medium; this is demonstrably true for rich galaxy clusters (e.g., Finoguenov et al. 2003). The concordance in mass breakdown between clusters and the Universe discussed above implies that, because of their deep potential wells, clusters, unlike most, if not all, galaxies, are "closed boxes" in the chemical evolution sense. Thus, modelers are provided with an unbiased and complete set of abundances that enables extraction of robust constraints on the stellar population responsible for metal enrichment.

For high temperatures, such as those found in the ICM, the shape of the thermal continuum emission yields a direct measurement of the electron temperature, and thus the ionization state. Complications arising from depletion onto dust grains, optical depth effects, and uncertain ionization corrections are minimal or absent. The energies of K-shell ($\rightarrow n = 1$) and/or L-shell ($\rightarrow n = 2$) transitions for *all* of the abundant elements synthesized after the era of Big Bang nucleosynthesis lie at wavelengths accessible to modern X-ray astronomical telescopes and instruments. The strongest ICM emission lines arise from well-understood H- and He-like ions, and line strengths are immediately converted into elemental abundances via spectral fitting. Of course, the quality and usefulness of X-ray spectra are limited by the available sensitivity and spectral resolution. In the following sections, I detail how the rapid progression in the capabilities of X-ray spectroscopy drives the evolution of our understanding of intracluster enrichment and its ultimate origin in primordial star formation in cluster galaxies. New puzzles are revealed with every insight emerging from subsequent generations of X-ray observatories, a situation that will surely continue with future missions.

1.2 Earliest Results on Cluster Enrichment

The 6.7 keV He-like Fe Kα emission line is the most easily detectable feature in ICM X-ray spectra, because it arises from a high-oscillator strength transition in an abundant ion and lies in a relatively isolated wavelength region. It was first detected in the *Ariel V* spectrum of the Perseus cluster (Mitchell et al. 1976), and *OSO-8* observations of the Perseus, Coma, and Virgo Clusters (Serlemitsos et al. 1977). Spectroscopic analysis of ~ 30 clusters (many observed with the *HEAO-1 A-2* satellite) revealed the ubiquity of this feature at a strength generally indicating an ICM Fe abundance of one-third to one-half solar (Mushotzky 1984). These early results demonstrated the origin of cluster X-ray emission as a thermal primordial plasma enriched by material processed in stars and ejected in galactic winds. Although not immediately realized, this provided the first indications of the prodigious magnitude of galactic outflows, since the measured amount of ICM Fe was of the same order as the sum of the Fe in all of the stars in all of the cluster galaxies.

Prior to 1993, Fe was the only element accurately measured in a large number of clusters, although some pioneering measurements of O, Mg, Si, and S features were obtained with the Solid State Spectrometer and Focal Plane Crystal Spectrometer aboard the *Einstein* X-ray Observatory (see Sarazin 1988 and references therein for these results, as well as a complete survey of the field prior to the the launch of the *ROSAT* and *Advanced Satellite for Cosmology and Astrophysics (ASCA)* X-ray observatories). Given the ambiguous origins of Fe, known to be synthesized in comparably large quantities by both Type Ia and Type II supernovae (henceforth, SNe Ia and SNe II) integrated over the history of the Milky Way, this represented a serious impediment to interpreting the data in terms of star formation history. Fortunately, the launch of *ASCA* provided the means to utilize the ICM as a repository of information on historical star formation and element creation.

1.3 ICM Abundances from the *ASCA* Database

With the combination of modest imaging capability, good spectral resolution, and large collecting area over a broad X-ray bandpass realized by its four telescope/detector pairs, the *ASCA* X-ray Observatory ushered in a new era of X-ray spectroscopy of astrophysical plasmas and revolutionized cluster elemental abundance studies (Arnaud et al. 1994; Bautz et al. 1994; Fukazawa et al. 1994). The clusters with accurate Fe abundance determinations cover a range of redshifts out to $z \approx 0.5$. This enabled the first investigation of the evolution of [Fe/H], as needed to understand the epoch and mechanism of enrichment (Mushotzky & Loewenstein 1997). The first results on gradients in ICM metallicity and abundance ratios were obtained (see §1.5), and the first significant sample of α-element abundances were measured with *ASCA*. Well over 400 observations of galaxy clusters and groups were made over the 1993–2000 duration of the *ASCA* mission. Because the *ASCA* data archive is now complete, and a comparable database based on observations with the current generation of X-ray observatories is many years away, an assessment of *ASCA* ICM enrichment results is timely.

The *ASCA* Cluster Catalog (ACC) project (Horner et al. 2004), initiated by K. Gendreau (NASA/GSFC), is the subject of the University of Maryland Ph.D. theses of D. Horner and W. Baumgartner, and includes contributions from R. Mushotzky, C. Scharf, and the author. Its overarching goal is to perform uniform and semi-automated spectral analysis on the integrated X-ray emission from every target in the *ASCA* cluster observational database, utilizing the most current processing and calibration. *ASCA* observed 434 galaxy clusters and groups in 564 pointings. Among these, 273 clusters are deemed suitable for spectroscopy, superseding previous samples (e.g., White 2000) by more than a factor of 2.

1.3.1 Fe Abundance Trends

The Fe abundance shows a remarkable uniformity in rich clusters, with a distribution that sharply peaks at ~ 0.4 solar (where solar Fe abundance is defined such that log (Fe/H) + 12 = 7.5; Grevesse & Sauval 1998). The Fe abundance tends to be higher in clusters with the highest central densities and shortest cooling times (see also Allen & Fabian 1998). It is unclear from these data alone whether this is an artifact of the presence of Fe gradients: since the X-ray emissivity is proportional to the gas density squared, X-ray spectra of more concentrated ICM are disproportionately weighted toward the more abundant central regions. There are also systematic trends with electron temperature, with Fe tending to be overabundant with respect to the average defined by the hottest clusters, for clusters with ICM temperatures 2 keV $< kT <$ 4 keV, and underabundant for $kT < 2$ keV.

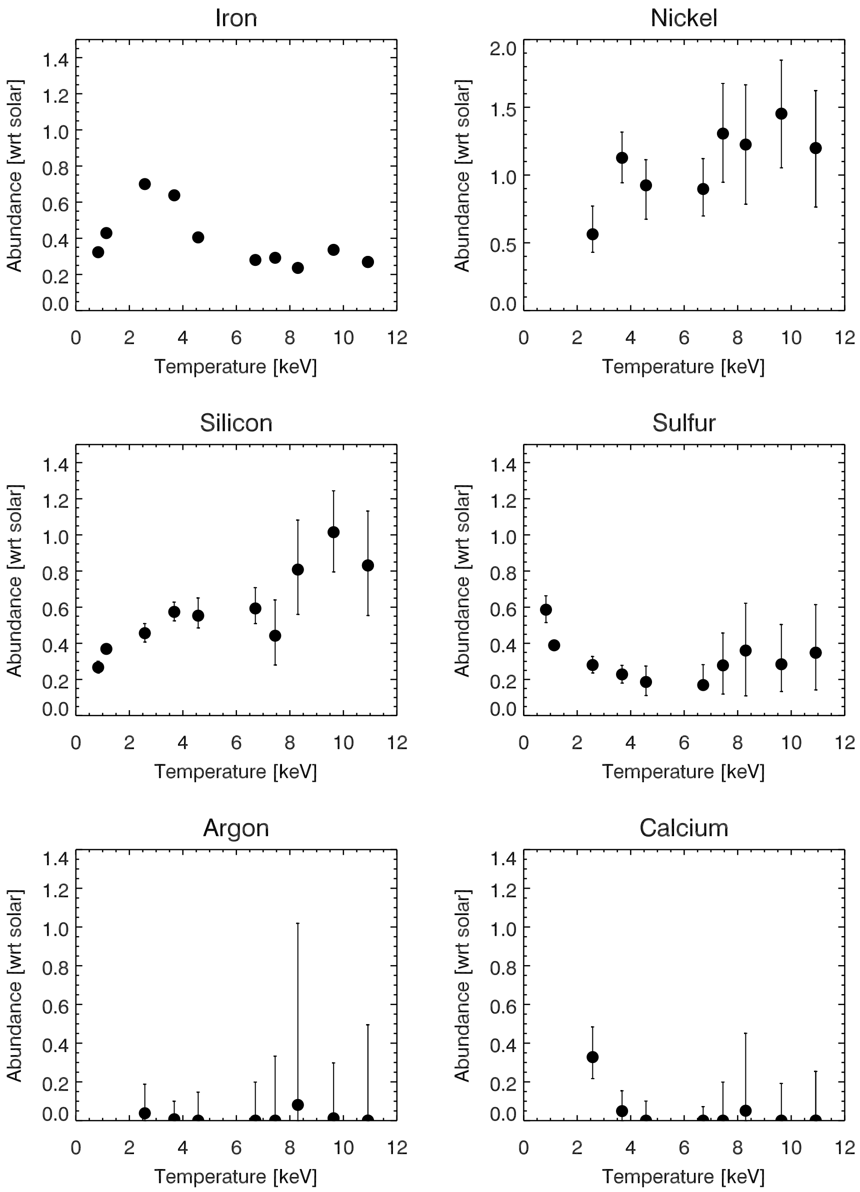

Fig. 1.1. Average abundances with respect to the solar abundances of Grevesse & Sauval (1998) as a function of temperature. 90% confidence errors are shown. (From Baumgartner et al. 2004.)

ASCA data revealed evidence for a *lack* of evolution in Fe abundance out to redshift 0.4 (Mushotzky & Loewenstein 1997; Rizza et al. 1998; Matsumoto et al. 2000, 2001) and no evidence of a decline at higher redshift (Donahue et al. 1999). *XMM-Newton* and *Chandra* measurements are further expanding the redshift range of precise cluster Fe abundance measurements (Jeltema et al. 2001; Arnaud et al. 2002; Maughan et al. 2003; Tozzi et al. 2003). On average, rich cluster Fe abundances are invariant out to $z \approx 0.8$, and show no sign of decline out to $z \approx 1.2$. The epoch of cluster enrichment is yet to be identified. Most of the star formation in the Universe occurred at $z > 1$ (Madau et al. 1996; Lanzetta et al. 2002; Dickinson et al. 2003), and fundamental plane considerations imply that most stars in clusters formed at $z > 2$ (van Dokkum et al. 1998; Jørgensen et al. 1999). Therefore, one expects *synthesis* of most cluster metals prior to the redshifts where they can presently be observed. However, it does not necessarily follow that the metals are in place in the ICM at such early epochs. As observations push back the enrichment era, scenarios where ICM metal injection from galaxies rapidly follows their synthesis during the early period of active star formation are favored over those with delayed metal release from galaxies, for example, via ongoing SN Ia-driven winds or stripping of enriched galaxy gas halo.

1.3.2 Metallicities, Abundance Patterns, and their Interpretation

Although often blended, emission features from O, Ne, Mg, Si, S, Ar, Ca, Fe, and Ni were measured in *ASCA* spectra of individual clusters. However, most of these are not detectable for the vast majority of the 273 observed systems. In order to obtain abundances with small statistical uncertainties, and smooth over both instrumental and astrophysical systematic effects and biases, Baumgartner et al. (2004) undertook joint analyses of multiple observations grouped into "stacks" of 13–47 clusters (Baumgartner et al. 2004) according to temperature (11 keV-wide bins centered on temperatures from 0.5–10.5 keV) and metallicity (high- and low-abundance bins). Ultimately, the two abundance stacks were merged for each temperature, and mean Si, S, Ar, Ca, Fe, and Ni abundances proved robust and reliable.

The results of the stacking analysis are summarized as follows (Fig. 1.1). For rich clusters ($kT > 4$ keV), the ratio of Si to Fe is $1.5-3$ times solar and displays an increasing trend with temperature. However, in contrast, the S-to-Fe ratio is solar or less (i.e. Si/S ≈ 3 times solar), and Ar and Ca are markedly subsolar with respect to Fe. The Ni-to-Fe ratio is $3-4$ times solar in these systems. This confirms and generalizes previous results (Mushotzky et al. 1996; Fukazawa et al. 1998; Dupke & White 2000a; Dupke & Arnaud 2001). Intermediate-to-poor clusters (2 keV $< kT <$ 4 keV) have subsolar ratios of both Si and S, with respect to Fe; however, the Si-to-S ratio remains high at about twice solar. This trend with temperature was previously identified by Fukazawa et al. (1998) and by Finoguenov, David, & Ponman (2000). The trend of higher α/Fe ratios in the hotter clusters with lower Fe/H (Fig. 1.2) is reminiscent of trends in Galactic stars and suggests the existence of ICM enrichment by a stellar population that is itself promptly enriched (i.e. by SNe II), as inferred for stars in bulges and elliptical galaxies.

Baumgartner et al. (2004) compare these ratios with those in various other systems, including the Galactic thin (Fig. 1.3) and thick disks, damped Lyα systems, Lyman-break galaxies, and the Lyα forest. In general, the high Si/Fe is not out of line with other systems of comparable Fe/H inferred to undergo rapid and efficient conversion of gas into stars. However, the low ratios of Ca to Fe and S to Si, and the high ratio of Ni to Fe evidently are unique to the ICM: a clear analog among observed classes of systems to the population responsible for enriching the ICM is not evident.

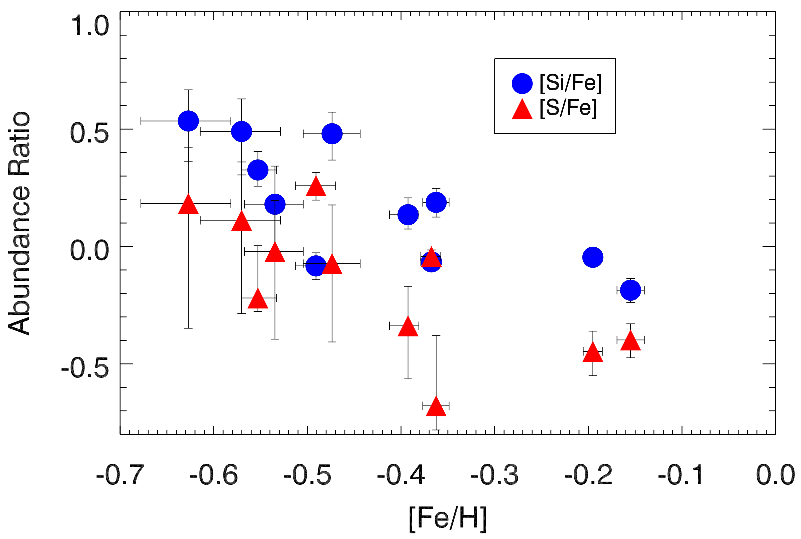

Fig. 1.2. Si/Fe and S/Fe ratios vs. Fe/H ratio, expressed as the logarithm with respect to solar. (From Baumgartner et al. 2004.)

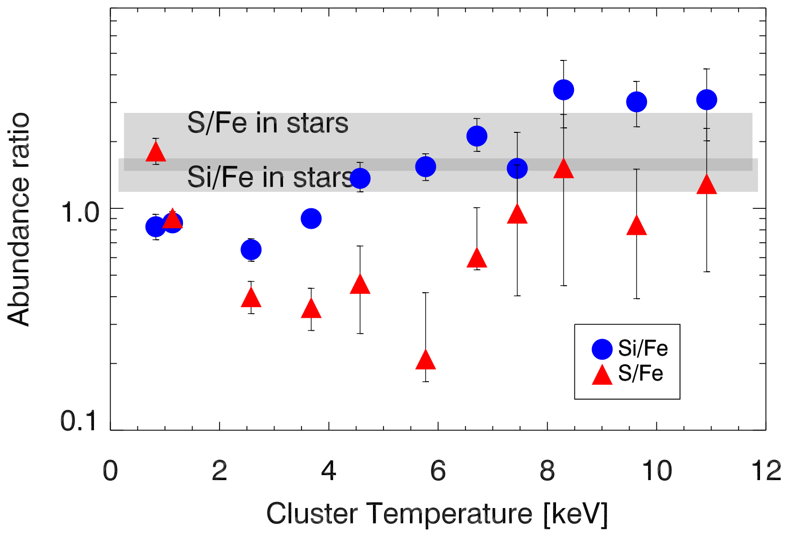

Fig. 1.3. Si/Fe and S/Fe ICM abundances vs. kT compared to those found in the Milky Way from Timmes, Woosley, & Weaver (1995). The range of Galactic Si/Fe is illustrated with the lower shaded rectangle, S/Fe with the upper, overlapping rectangle (Baumgartner et al. 2004).

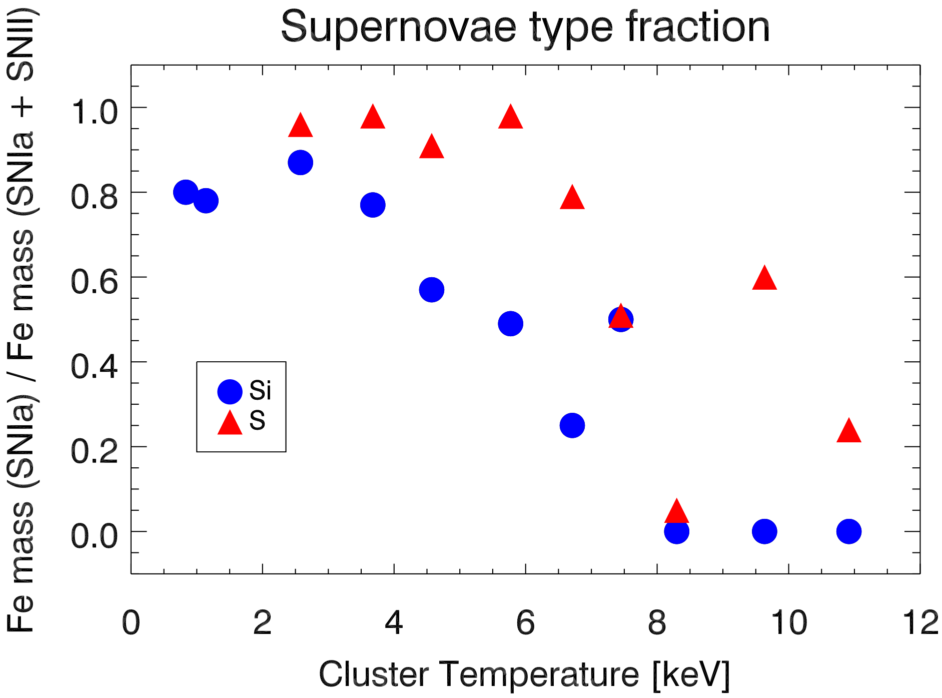

Fig. 1.4. Decomposition into SNe Ia and SNe II, using standard yields and the observed Si/Fe and S/Fe ratios, expressed in terms of the fraction of Fe from SNe Ia. (From Baumgartner et al. 2004.)

1.4 On the ICM Abundance Anomalies

Since bulges account for $\sim 90\%$ of the stellar mass in clusters, it is straightforward to estimate ICM enrichment under standard assumptions. Consider a simple stellar population with a local IMF (e.g., Kroupa 2001), assume that stars more massive than 8 $M_\odot$ explode as SNe II, that the rate of SN Ia explosions is as determined in nearby elliptical galaxies (0.16 SNU, where 1 SNU $\equiv$ 1 SN per 10^{10} solar blue luminosities per century; Cappellaro, Evans, & Turatto 1999) and injected for a duration of 10^{10} yr, and utilize SNe II and SNe Ia ("W7" model) yields from Nomoto et al. (1997a, b) with the former averaged over a standard IMF extending to 40 $M_\odot$ as in Thielemann, Nomoto, & Hashimoto (1996). The fractions of Fe originating in SNe Ia separately inferred from the Si/Fe and S/Fe ratios are shown in Figure 1.4, illustrating that *no* combination of standard SNe Ia and SNe II can explain the ICM abundance pattern. Baumgartner et al. (2004) demonstrate that this holds regardless of which published SN II yields are considered (see also Gibson, Loewenstein, & Mushotzky 1997; Loewenstein 2001).

In addition to ratios, it is instructive to consider the ICM mass in metals, normalized to the total starlight in cluster galaxies. Table 1.2 compares the mass-to-light ratios of the elements addressed in the stacking analysis, computed using the standard assumptions detailed above, with the observed averages in three ICM temperature regimes. The predicted SN II and SN Ia

Table 1.2. *Metal Mass-to-Light Ratios*

	Predicted				Observed		
	SNe II	SNe Ia W7	SNe Ia WDD1	SNe II W7	$kT > 8$ (keV)	$4 < kT < 8$ (keV)	$2 < kT < 4$ (keV)
Si	9.3×10^{-3}	2.4×10^{-4}	5.6×10^{-4}	9.3×10^{-3}	2.3×10^{-2}	1.3×10^{-2}	7.5×10^{-3}
S	3.1×10^{-3}	1.4×10^{-4}	3.4×10^{-4}	3.3×10^{-3}	4.5×10^{-3}	2.5×10^{-3}	2.3×10^{-3}
Ar	6.1×10^{-4}	2.6×10^{-4}	6.9×10^{-5}	6.3×10^{-4}	$< 9.6 \times 10^{-4}$	$< 5.5 \times 10^{-4}$	...
Ca	4.5×10^{-4}	2.0×10^{-4}	6.5×10^{-5}	4.7×10^{-4}	$< 6.6 \times 10^{-4}$	$< 3.8 \times 10^{-4}$	...
Fe	6.9×10^{-3}	1.2×10^{-3}	8.7×10^{-4}	8.1×10^{-3}	1.4×10^{-2}	1.5×10^{-2}	1.7×10^{-2}
Ni	4.5×10^{-4}	2.3×10^{-4}	5.7×10^{-5}	6.8×10^{-4}	3.1×10^{-3}	2.7×10^{-3}	...

contributions are shown separately, as well as their sum. For comparison, the predictions for a delayed detonation SN Ia model ("WDD1," Nomoto et al. 1997b) are shown along with those using the standard W7 model; use of the former generally exacerbates the problems detailed below.

There are a number of notable discrepancies. Both Fe and Ni are generally underpredicted, as is Si at high temperatures. One could achieve reconciliation for Fe and Si by roughly doubling the numbers of SNe Ia and SNe II, alterations that are not unreasonable since the SN Ia rate may be greater in the past and the IMF may be top-heavy (flat or bimodal; e.g., Loewenstein & Mushotzky 1996). One could then, perhaps, explain the Si/Fe trend with ICM temperature as selective mass loss of SN II products in systems with shallower gravitational potential wells. However, such a scenario overpredicts S, Ar, and Ca and underpredicts Ni.

The large observed amounts of Ni require a SN Ia rate, averaged over a Hubble time, of more than 10 times the estimated local rate, with a concomitant decrease in the number of SNe II to avoid overproducing Fe. However, this underpredicts Si. The problem is intractable using standard yields, unless a significant additional source of metals is considered.

What are some possible resolutions to this puzzle? The only explanation for the high Ni abundance is a high time-averaged SN Ia rate and/or a high SN Ia Ni yield—the rate must exceed $\sim 2(0.14/y_{\rm Ia,Ni})$ SNU, where $y_{\rm Ia,Ni}$ is the SN Ia Ni yield in solar masses. To account for those systems with high Si abundances, one could assume that SN II Si yields are twice those in the core collapse nucleosynthesis calculations currently in the literature. Alternatively, the Si overabundance could be explained if the number of massive SN II progenitor stars were approximately twice what a standard IMF predicts; but, in this case the S, Ar, Ca, and, perhaps, Fe yields require *ad hoc* reduction to avoid their overproduction.

If published yields are not grossly in error, one must appeal to an additional source of enrichment that preferentially synthesizes Si. These progenitors must be more plentiful, or their products more efficiently retained, in more massive clusters. An extensive search of the literature reveals several instances of SNe with the desired yield-pattern, including core collapse SN from very massive (70 $M_\odot$) stars (Thielemann et al. 1996), massive ($\sim$ 30 $M_\odot$) metal-poor ($\sim$ 0.01 solar) stars (Woosley & Weaver 1995), or supermassive (with 70 $M_\odot$ He cores) metal-free stars that explode as hypernovae (Heger & Woosley 2002). While it is unlikely that a monolithic contribution from any of these objects truly explains

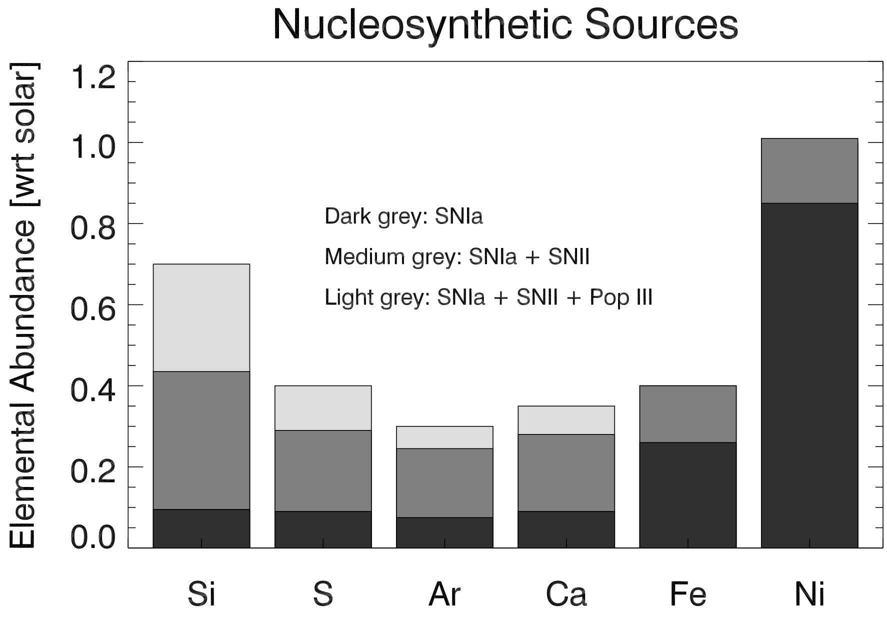

Fig. 1.5. Relative contributions to the enrichment of various elements in a typical clusters for a toy model including Population III hypernovae in addition to SNe Ia and SNe II in standard numbers with standard yields (Baumgartner et al. 2004).

the ICM abundance anomalies, their existence demonstrates that there are nucleosynthetic channels—likely associated with very massive and/or very metal-poor stars—that result in relative enhancements of Si. Figure 1.5 shows the respective contributions of SNe Ia, SNe II, and hypernovae (Heger & Woosley 2002) to each element in a toy model that reproduces a typical rich cluster ICM abundance pattern (Baumgartner et al. 2004).

There are now possible signatures of Population III and hypernovae in the level and pattern of enrichment in low-metallicity Milky Way stars (Umeda & Nomoto 2003), in the level and epoch of intergalactic medium enrichment as inferred from the Lyα forest (Songaila 2001), and in the reionization of the Universe (e.g., Wyithe & Loeb 2003). The number of hypernovae required in the ICM is reasonable in terms of the expected number of Population III progenitors (Loewenstein 2001).

1.5 *Chandra* and *XMM-Newton* Results on Abundance Gradients

ASCA data revealed clear evidence of central excesses of Fe in clusters with cooling flows and in clusters not involved in recent major mergers (Matsumoto et al. 1996; Ezawa et al. 1997; Ikebe et al. 1997, 1999; Xu et al. 1997; Kikuchi et al. 1999; Dupke & White 2000a, b), which are consistent with generally flat metallicity profiles outside of the central $\sim 2'$ (Tamura et al. 1996; Irwin, Bregman, & Evrard 1999; White 2000). Limitations in *ASCA* imaging precluded resolving gradients in Fe or drawing robust conclusions on the spatial distribution of α/Fe ratios, although there were indications that α elements may not display the central excess (Finoguenov et al. 2000; Fukazawa et al. 2000; Allen et al. 2001). *BeppoSAX* provided Fe profiles with better spatial resolution, and De Grandi & Molendi (2001) attributed the central Fe excess to injection by SNe Ia associated with the stellar population in the central cluster galaxy. If this is the case, milder or absent central excesses in SN II-synthesized α elements are expected, as claimed by Finoguenov et al. (2000).

These questions of gradients in abundance ratios are addressed through observations with the *Chandra* (Weisskopf et al. 2002) and *XMM-Newton* (Jansen et al. 2001) X-ray observatories. The former represents a huge leap in broad-bandpass imaging, with an angular resolution $\sim 0.''5$, the latter in collecting area (a total of ~ 5 times that of *ASCA*, with an order of magnitude better angular resolution). New results demonstrate that the central Fe excess is concentrated to within 100 kpc of the cluster center (Iwasawa et al. 2001; Kaastra et al. 2001; Lewis, Stocke, & Buote 2002; Smith et al. 2002), that there may be a central metallicity inversion (Johnstone et al. 2002; Sanders & Fabian 2002; Schmidt, Fabian, & Sanders 2002; Blanton, Sarazin, & McNamara 2003; Dupke & White 2003), and that abundance profiles are generally very flat from ~ 100 kpc out to a significant fraction of the virial radius (Schmidt, Allen, & Fabian 2001; Tamura et al. 2001). The apparent inversion may be an artifact of using an oversimplified model in spectral fitting (Molendi & Gastaldello 2001). The question of the presence of α/Fe gradients is not yet definitively settled (David et al. 2001), although early results indicate a mix of abundances in the central regions that is closer to the SN Ia pattern than is globally the case (Tamura et al. 2001; Ettori et al. 2002).

1.6 *XMM-Newton* RGS Measurements of CNO

The *XMM-Newton* Reflection Grating Spectrometer provides high-spectral resolution ($E/\Delta E$ ranges from 200 to 800 over the 0.35–2.5 keV RGS bandpass; den Herder et al. 2003) spectroscopy in the wavelength region containing the strongest X-ray features of the elements carbon through sulfur. Since individual lines are more distinctly resolved than in previous studies using CCD spectra (where $E/\Delta E \approx 50$), abundance determinations are much less sensitive to the assumed thermal emission model. C, N, and O lines are all widely accessible for the first time. These are unique probes of star formation and the era of ICM enrichment because of their distinctive nucleosynthetic origins. For an extended X-ray source such as a galaxy cluster, RGS spectra correspond to an emission-weighted average over the inner $\sim 1'$ (see Peterson et al. 2003)—within the central galaxy (if there is one) for a nearby cluster; thus, caution must be exercised in applying the results to the source as a whole.

1.6.1 Oxygen

The strong 0.65 keV OV III Lyα feature is measured with *XMM-Newton* in clusters out to redshifts as high as 0.3. The O/Fe ratio for the sample of cooling flow clusters in Peterson et al. (2003) is shown in Figure 1.6. [Note that Peterson et al. adopt the definition of solar abundances from Anders & Grevesse (1989), where log (Fe/H) + 12 = 7.67 and log (O/H) + 12 = 8.93, ~ 1.5 and ~ 1.7 times higher than currently more commonly used "cosmic abundances" of Fe and O, respectively.] O/Fe is generally subsolar, and overlaps with the range measured in Galactic stars of comparable Fe/H (Reddy et al. 2003). Low O abundances were previously reported in Abell 1795 (Tamura et al. 2001a), Abell 1835 (Peterson et al. 2001), Sèrsic 159-03 (Kaastra et al. 2001), Abell 496 (Tamura et al. 2001b),

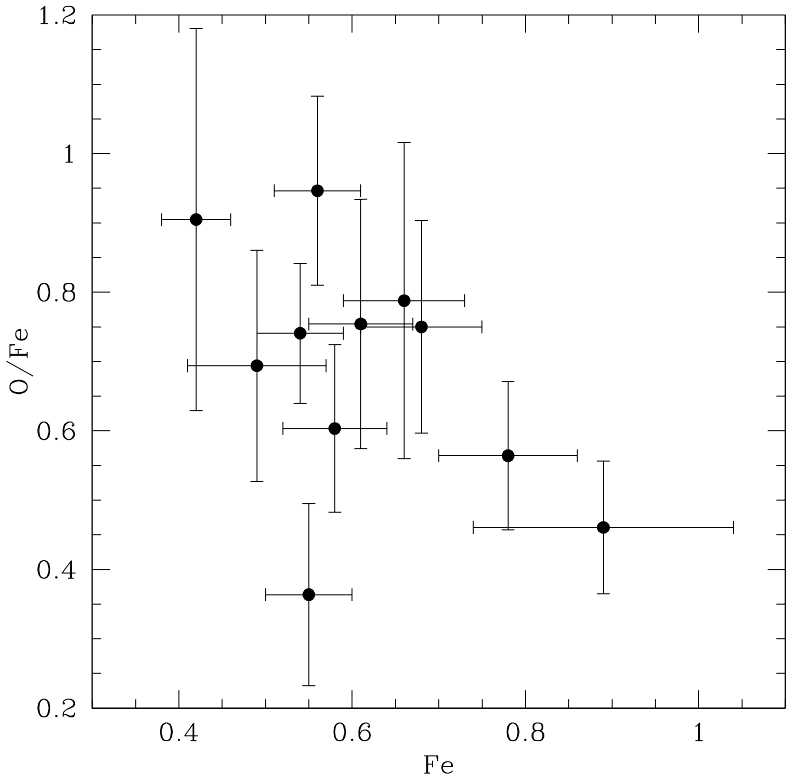

Fig. 1.6. O/Fe vs. Fe for cooling flow clusters. (Adapted from Peterson et al. 2003.)

NGC 5044, the central (elliptical) galaxy in the WP23 group (Tamura et al. 2003), and the elliptical galaxy NGC 4636 (Xu et al. 2002), which resembles a group in X-rays. The Galactic O/Fe-Fe/H trend is thought to reflect the delayed enrichment in Fe from SNe Ia relative to that of O from short-lived, massive SN II progenitors. In the intergalactic medium of clusters and groups, we may be seeing systematic variations in the relative stellar lock-up fractions of SN II and SN Ia products, relative retention of injected SN II and SN Ia material, or IMF. Low O/Si ratios in these systems were interpreted as a possible signature of enrichment by hypernovae associated with Population III (Loewenstein 2001). Intriguingly, as shown in Figure 1.7, Mg appears not be a good surrogate for O, as often assumed in studies of elliptical galaxies.

1.6.2 Carbon and Nitrogen

The Lyα lines of the H-like ions of C and N are weak compared to O, and fall in a less sensitive and less well-calibrated wavelength region of the RGS. As a result, there presently are few measurements of C and N: C and N in A 496 and M87 (Peterson et al. 2003) and N in the elliptical galaxies NGC 4636 (Xu et al. 2002) and NGC 5044 (Tamura et al. 2003). N is of particular interest, since its origin in intermediate-mass stars provides

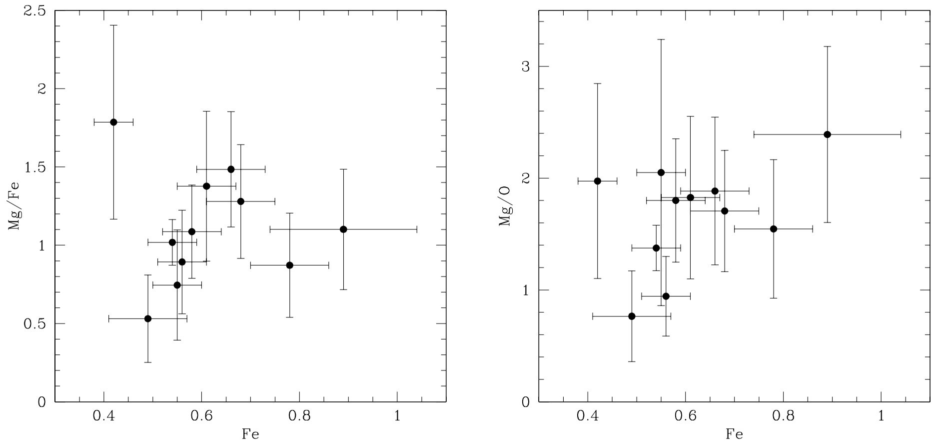

Fig. 1.7. Mg/Fe and Mg/O vs. Fe for cooling flow clusters. (From Peterson et al. 2003.)

crucial leverage in distinguishing the mass function of the enriching stellar population. In these objects C (when measured) and N are ∼solar, and C/O and N/O are ∼twice solar [solar as in Anders & Grevesse 1989: loG(C/H) + 12 = 8.56, log (N/H) + 12 = 8.05]. On a plot of N/O vs. O/H, these systems overlap with measurements in extragalactic H II regions (Pettini et al. 2002), where the secondary production of N dominates, but do extend to somewhat higher N/O at the same O/H.

1.7 *XMM-Newton* Observations of M87

Because of its brightness, M87 in the Virgo cluster is among the most extensively X-ray spectroscopically studied extended extragalactic objects. Its proximity enables one to extract detailed plasma conditions and composition, and to evaluate and correct for systematic effects. Previous work based on spectra from the *Einstein* (Canizares et al. 1982; Stewart et al. 1984; White et al. 1991; Tsai 1994a, b), *ROSAT* (Nulsen & Bohringer 1995; Buote 2001), and *ASCA* (Matsumoto et al. 1996; Hwang et al. 1997; Buote, Canizares, & Fabian 1999; Finoguenov & Jones 2000; Shibata et al. 2001) observatories is rapidly becoming superseded by *Chandra* and *XMM-Newton* data.

The RGS results for M87 show that, in the inner ~ 10 kpc, abundances of C, N, Ne, and Mg have best-fit values (relative to Anders & Grevesse 1989) of 0.7–1.0 solar, with 90% uncertainties of 0.2–0.3, while Fe is 0.77 ± 0.04 solar, and O 0.49 ± 0.04 solar (Sakelliou et al. 2002). With respect to the M87 stellar abundances (Milone, Barbuy, & Schiavon 2000), the α elements are apparently preferentially diluted with respect to Fe.

Gastaldello & Molendi (2002) derive detailed abundance distributions from analysis of *XMM-Newton* EPIC-MOS CCD data, obtaining O, Ne, Mg, Si, Ar, Ca, Fe, and Ni in 10 radial bins extending to $14'$. The MOS results are generally consistent with the RGS and indicate negative gradients on arcminute scales in all of the elements, with the possible exception of Ne. Gradients in α/Fe ratios are modest. Ratios with respect to Fe vary among the α elements: O/Fe, Ne/Fe, Mg/Fe, and S/Fe are subsolar; Si/Fe, Ar/Fe, and Ca/Fe are slightly supersolar. Ni/Fe increases from ~ 1.5 solar in the center to ~ 2.5 solar at 50 kpc.

Not surprisingly, Gastaldello & Molendi find that no unique combination of published SN Ia (either deflagration or delayed detonation models) and SN II yields is consistent with the full abundance pattern at any radius. Moreover, the combination of SN subtypes that provides the best fit varies with radius (i.e. delayed detonation models provide a better fit in the center, W7 further out where Ni/Fe is greater).

Finoguenov et al. (2002) utilize a cruder spatial division, thus obtaining higher precision for individual abundances (this is enhanced by their inclusion of *XMM-Newton* EPIC-PN CCD data). They propose explaining the observed abundance pattern and its radial variation with (1) a radially increasing SN II/SN Ia ratio, (2) high Si and S yields from SNe Ia (favoring delayed detonation models) and an *ad hoc* reduction in SN II S yields, and (3) a radial variation in SN Ia yields (corresponding to delayed detonation models with different deflagration-to-detonation transition densities). As they note, deflagration models must also play a role to account for the high Ni/Fe ratio found in other clusters. Whether such a complex model can coherently explain cluster abundance patterns in general is unclear. Matsushita, Finoguenov, & Bohringer (2003) follow this up with more sophisticated thermal modeling, and an analysis that includes individual line ratios, and they reach conclusions that are qualitatively similar in terms of the outwardly increasing importance of SNe II, the diversity of SNe Ia, and the yields of Si and S.

It is important to keep in mind that these new results are for the central ~ 70 kpc—still well within the influence of the M87 galaxy. The larger-scale cluster plasma (as studied in the ACC project discussed above) is not as profoundly affected by SNe Ia, and, indeed, there are indications of a transition to a more cluster-like abundance pattern at large radii in M87 (Finoguenov et al. 2002). In fact, the narrowing redshift window when the Fe in clusters must be synthesized and mixed into the ICM, as inferred from the lack of Fe abundance evolution, is becoming comparable to the time delay characteristic of many models of SN Ia explosions.

1.8 Concluding Remarks

The era of high-precision X-ray spectroscopy has arrived. Accurate and robust measurements can now be made of abundances and their variation in space and time, for a wide variety of elements in intracluster and intragroup media. This enables astronomers to utilize the ICM, where metals synthesized in cluster galaxy stars over the age of the Universe accumulated, as a laboratory for testing theories of the environmental dependence and impact of star formation.

1.8.1 Mean ICM Metallicities and Redshift Dependence

There are now hundreds of measurements, out to redshifts greater than 1, of Fe abundances and many tens of measurements (or significant upper limits) of Si, S, Ar, Ca, and Ni. The distribution function of Fe abundance outside of the central regions in rich clusters is sharply peaked around ~ 0.4 solar, and shows no evidence of a decline with increasing redshift out to $z \approx 1$. With the average Fe yield per current mass of stars ~ 3 times solar, a prodigious rapid enrichment is implied: a time average of $\sim 0.1\ M_{\odot}\ \mathrm{yr}^{-1}$ of Fe per (present-day) L_* galaxy integrated over 2 Gyr. This is equivalent to the nucleosynthetic yield of ~ 1 SN II yr^{-1} per L_* galaxy, corresponding to $\sim 100\ M_{\odot}\ \mathrm{yr}^{-1}$ per L_* galaxy forming stars with a Salpeter IMF, or ~ 20 SNU of SNe Ia! As a point of reference, note that the mean star formation rate in the Universe at high redshift, normalized to the cluster light, is ~ 0.02

$M_{\odot}$ yr^{-1} per L_* galaxy. So, despite a stellar fraction consistent with the universal average, several times the amount of metals that might be expected was synthesized in clusters. It is intriguing that Lyman-break galaxies were enriched to similar levels on a comparably brief time interval. In the extreme overdense regions that represent clusters of galaxies, the primordial IMF was skewed toward high masses, or an additional separate primordial population of massive stars was present. Clusters are thus strong candidates for the source of the missing metals at $z \approx 3$ (Finoguenov et al. 2003), even though only about 5% of the total universal baryon content resides in clusters.

1.8.2 Abundance Gradients

Centrally concentrated ($<$ 100 kpc) excesses in Fe are common, and evidently exclusively occur in those clusters that can be characterized either as cooling flow clusters, as clusters with a massive central galaxy, or as clusters without recent major merging activity. An explanation of this phenomenon awaits additional *Chandra* and *XMM-Newton* results on the radial distribution of α elements. Early indications are that SNe Ia play a more important role at the location of central cluster galaxies, although other giant elliptical galaxies evidently did not retain such large masses of interstellar Fe. Metallicity gradients evidently are mild or absent beyond these central regions.

1.8.3 Abundance Patterns

There is more Si, Fe, and Ni than one might expect based on the observed stellar population. The relative abundances of elements measured in the ICM show clear departures from solar ratios and the abundance pattern in the Galactic disk and other well-studied galactic and protogalactic systems. The ICM abundance pattern shows systematic variations with ICM temperature (i.e. cluster gravitational potential well depth). These variations are apparent even in the relative abundances, which are not generally in solar ratios, among different α elements (O, Mg, Si, S, Ar, and Ca). Contribution from an additional, primordial source of metals may be required to finally explain these anomalies. The ICM Ni/Fe ratio is $2-4$ times solar, higher than in any other known class of object where this ratio is measured. Since both Fe and Ni are efficiently synthesized in SNe Ia, and given the importance of SNe Ia as fundamental probes of the cosmological world model, the origin of the Ni excess is clearly worthy of further investigation.

1.8.4 The Future

As the *Chandra* and *XMM-Newton* cluster databases mature, one can expect many more measurements of abundance gradients (of α elements, as well as Fe), tight constraints on the evolution of Si and O abundances out to $z > 0.4$ and Fe out to $z > 1$, and additional accurate measurements of C and N. *ASTRO-E2*, scheduled for launch in 2005, will provide true spatially resolved, high-resolution X-ray spectroscopy, which will yield cleaner measurements of N, O, Mg, and Ne, and their gradients.

Acknowledgements. I would like to acknowledge the organizers for their kind invitation to participate in this meeting, and for all of their efforts in assembling the conference and these proceedings. My gratitude extends to Richard Mushotzky and Wayne Baumgartner for their assistance in preparing this review.

References

Allen, S. W., & Fabian, A. C. 1998, MNRAS, 297, L63
Allen, S. W., Fabian, A. C., Johnstone, R. M., Arnaud, K. A., & Nulsen, P. E. J. 2001, MNRAS, 322, 589
Anders, E., & Grevesse, N. 1989, Geochim. Cosmochim. Acta, 53, 197
Arnaud, K. A. 1994, ApJ, 436, L67
Arnaud, M., et al. 2002, A&A, 390, 27
Bahcall, N. A., & Comerford, J. M. 2002, ApJ, 565, L5
Baumgartner, W. H., Loewenstein, M., Horner, D. J., & Mushotzky, R. F. 2004, ApJ, submitted
Bautz, M. W., Mushotzky, R., Fabian, A. C., Yamashita, K., Gendreau, K. C., Arnaud, K. A., Crew, G. B., & Tawara, Y. 1994, PASJ, 46, L131
Bell, E. F., McIntosh, D. H., Katz, N., & Weinberg, M. D. 2003, ApJ, 585, L117
Blanton, E. L., Sarazin, C. L., & McNamara, B. R. 2003, ApJ, 585, 227
Buote, D. A. 2001, ApJ, 548, 652
Buote, D. A., Canizares, C. R., & Fabian, A. C. 1999, MNRAS, 310, 483
Canizares, C. R., Clark, G. W., Jernigan, J. G., & Markert, T. H. 1982, ApJ, 262, 33
Cappellaro, E., Evans, R., & Turatto, M. 1999, A&A, 351, 459
Davé, R., et al. 2001, ApJ, 552, 473
David, L. P., Nulsen, P. E. J., McNamara, B. R., Forman, W., Jones, C., Ponman, T., Robertson, B., & Wise, M. 2001, ApJ, 557, 546
Davis, D. S., Mulchaey, J. S., & Mushotzky, R. F. 1999, ApJ, 511, 34
De Grandi, S., & Molendi, S. 2001, ApJ, 551, 153
den Herder, J.-W., et al. 2003, SPIE, 4851, 196
Dickinson, M., Papovich, C., Ferguson, H. C., & Budavàri, T. 2003, ApJ, 587, 25
Donahue, M., Voit, G. M., Scharf, C. A., Gioia, I. M., Mullis, C. R., Hughes, J. P., & Stocke, J. T. 1999, ApJ, 527, 525
Dupke, R. A., & Arnaud, K. A. 2001, ApJ, 548, 141
Dupke, R. A., & White, R. E. III 2000a, ApJ, 528, 139
——. 2000b, ApJ, 537, 123
——. 2003, ApJ, 583, L13
Ettori S., & Fabian A. C. 1999, MNRAS, 305, 834
Ettori S., Fabian A. C., Allen, S. W., & Johnstone, R. M. 2002, MNRAS, 305, 834
Evrard, A. E. 1997, MNRAS, 292, 289
Ezawa, H, Fukazawa, Y., Makishima, K., Ohashi, T., Takahara, F, Xu, H., & Yamasaki, N. Y. 1997, ApJ, 490, L33
Finoguenov, A., Burkert, A., & Bohringer, H. 2003, ApJ, 594, 136
Finoguenov, A., David, L. P., & Ponman, T. J. 2000, ApJ, 544, 188
Finoguenov, A., & Jones, C. 2000, ApJ, 539, 603
Finoguenov, A., Matsushita, K., Bohringer, H., Ikebe, Y., & Arnaud, M. 2002, A&A, 381, 21
Fukazawa, Y., et al. 1998, PASJ, 50, 187
Fukazawa, Y., Makishima, K., Tamura, T., Nakazawa, K., Ezawa, H., Ikebe, Y., Kikuchi, K., & Ohashi, T. 2000, MNRAS, 313, 21
Fukazawa, Y., Ohashi, T., Fabian, A. C., Canizares, C. R., Ikebe, Y., Makishima, K., Mushotzky, R. F., & Yamashita, K. 1994, PASJ, 46, L55
Fukugita, M., Hogan, C. J., & Peebles, P. J. E. 1998, ApJ, 312, 518
Gastaldello, F., & Molendi, S. 2002, ApJ, 572, 160
Gibson, B. K., Loewenstein, M., & Mushotzky, R. F. 1997, MNRAS, 290, 623
Girardi, M., Manzato, P., Mezzetti, M., Giuricin, G., & Limboz, F. 2002, ApJ, 569, 720
Grevesse, N., & Sauval, A. J. 1998, Space Science Reviews, 85, 161
Heger, A., & Woosley, S. E. 2002, ApJ, 567, 532
Horner, D. J., et al. 2004, ApJS, submitted
Hwang, U., Mushotzky, R. F., Burns, J. O., Fukazawa, Y., & White, R. A. 1999, ApJ, 516, 604
Hwang, U., Mushotzky, R. F., Loewenstein, M., Markert, T. H., Fukazawa, Y., & Matsumoto, H. 1997, ApJ, 476, 560
Ikebe, Y., et al. 1997, ApJ, 481, 660
Ikebe, Y., Makishima, K., Fukazawa, Y., Tamura, T., Xu, H., Ohashi, T., & Matsushita, K. 1999, ApJ, 525, 58
Irwin, J. A., Bregman, J. N., & Evrard, A. E. 1999, ApJ, 519, 518
Iwasawa, K., Fabian, A. C., Allen, S. W., & Ettori, S. 2001, MNRAS, 328, L5
Jansen, F., et al. 2001, A&A, 365, L1

Jeltema, T. E., Canizares, C. R., Bautz, M. W., Malm, M. R., Donahue, M., & Garmire, G. 2001, ApJ, 562, 124
Johnstone, R. M., Allen, S. W., Fabian, A. C., & Sanders, J. S. 2002, MNRAS, 336, 299
Jørgensen, I., Franx, M., Hjorth, J., & van Dokkum, P. G. 1999, MNRAS, 308, 833
Kaastra, J. S., Ferrigno, C., Tamura, T., Paerels, F. B. S., Peterson, J. R., & Mittaz, J. P. D. 2001, A&A, 365, L99
Kikuchi, K., Furusho, T., Ezawa, H., Yamasaki, N. Y., Ohashi, T., Fukazawa, Y., & Ikebe, Y. 1999, PASJ, 51, 301
Kroupa, P. 2001, MNRAS, 322, 231
Lanzetta, K. M., Yahata, N., Pascarelle, S., Chen, H.-W., & Fernández-Soto, A. 2002, ApJ, 570, 492
Lewis, A. D., Stocke, J. T., & Buote, D. A. 2002, ApJ, 573, L13
Lin, Y.-T., Mohr, J. J., & Stanford, S. A. 2003, ApJ, 591, 749
Loewenstein, M. 2001, ApJ, 557, 573
Loewenstein, M., & Mushotzky, R. F. 1996, ApJ, 466, 695
Madau, P., Ferguson, H. C., Dickinson, M. E., Giavalisco, M., Steidel, C. C., & Fruchter, A. 1996, MNRAS, 283, 1388
Madau, P., & Pozzetti, L. 2000, MNRAS, 312, L9
Matsumoto, H., Koyama, K., Awaki, H., Tomida, H., Tsuru, T., Mushotzky, R., & Hatsukade, I. 1996, PASJ, 48, 201
Matsumoto, H., Pierre, M., Tsuru, T. G., & Davis, D. 2001, A&A, 374, 28
Matsumoto, H., Tsuru, T. G., Fukazawa, Y., Hattori, M., & Davis, D. 2000, PASJ, 52, 153
Matsushita, K., Finoguenov, A., & Bohringer, H. 2003, A&A, 401, 443
Maughan, B. J., Jones, L. R., Ebeling, H., Perlman, E., Rosati, P., Frye, C., & Mullis, C. R. 2003, ApJ, 587, 589
Milone, A., Barbuy, B., & Schiavon, R. P. 2000, AJ, 120, 131
Mitchell, R. J., Culhane, J. L., Davison, P. J., & Ives, J. C. 1976, MNRAS, 175, 29p.
Mohr, J. J., Mathiesen, B., & Evrard, A. E. 1999, ApJ, 517, 627
Molendi, S., & Gastaldello, F. 2001, A&A, 375, L14
Mulchaey, J. S. 2000, ARA&A, 38, 289
Mushotzky, R. F. 1984, Phys. Scripta T7, 157
Mushotzky, R. F., & Loewenstein, M. 1997, ApJ, 481, L63
Mushotzky, R., Loewenstein, M., Arnaud, K. A., Tamura, T., Fukazawa, Y., Matsushita, K., Kikuchi, K., Hatsukade, I. 1996, ApJ, 466, 686
Nomoto, K., Hashimoto, M., Tsujimoto, T., Thielemann, F.-K., Kishimoto, N., Kubo, Y., & Nakasato, N. 1997a, Nuclear Physics A, 616, 79
Nomoto, K., Iwamoto, K., Nakasato, N., Thielemann, F.-K., Brachwitz, F., Tsujimoto, T., Kubo, Y., & Kishimoto, N. 1997b, Nuclear Physics A, 621, 467
Nulsen, P. E. J., & Bohringer, H. 1995, MNRAS, 274, 1093
Peterson, J. R., et al. 2001, A&A, 365, L104
Peterson, J. R., Kahn, S. M., Paerels, F. B. S., Kaastra, J. S., Tamura, T., Bleeker, J. A. M., Ferrigno, C., & Jernigan, J. G. 2003, ApJ, 590, 207
Pettini, M., Ellison, S. L., Bergeron, J., & Petitjean, P. 2002, A&A, 391, 21
Reddy, B. E., Tomkin, J., Lambert, D. L., & Allende Prieto, C. 2003, MNRAS, 340, 304
Rizza, E., Burns, J. O., Ledlow, M. J., Owen, F. N., Voges, W., & Bliton, M. 1998, MNRAS, 301, 328
Sakelliou, I., et al. 2002, A&A, 391, 903
Sanders, J. S., & Fabian, A. C. 2002, MNRAS, 331, 273
Sarazin, C. L. 1988, X-ray Emission from Clusters of Galaxies (Cambridge: Cambridge Univ. Press)
Schmidt, R. W., Allen, S. W., & Fabian, A. C. 2001, MNRAS, 327, 1057
Schmidt, R. W., Fabian, A. C., & Sanders, J. S. 2002, MNRAS, 337, 71
Schuecker, P., Bohringer, H., Collins, C. A., & Guzzo, L. 2003, A&A, 398, 867
Serlemitsos, P. J., Smith, B. W., Boldt, E. A.,Holt, S. S., & Swank, J. H. 1977, ApJ, 211, L63.
Shibata, R., Matsushita, K., Yamasaki, N. Y., Ohashi, T., Ishida, M., Kikuchi, K., Bohringer, H., & Matsumoto, H. 2001, ApJ, 549, 228
Smith, D. A., Wilson, A. S., Arnaud, K. A., Terashima, Y., & Young, A. J. 2002, ApJ, 565, 195
Songaila, A. 2001, ApJ, 561, L153 (erratum: 2002, 568, L139)
Spergel, D. N., et al. 2003, ApJS, 148, 175
Stewart, G. C., Fabian, A. C., Nulsen, P. E. J., & Canizares, C. R. 1984, ApJ, 278, 536
Tamura, T., et al. 1996, PASJ, 48, 671
——. 2001b, A&A, 365, L87
Tamura, T., Bleeker, J. A. M., Kaastra, J. S., Ferrigno, C., & Molendi, S. 2001a, A&A, 379, 107
Tamura, T., Kaastra, J. S., Makishima, K., & Takahashi, I. 2003, A&A, 399, 497

Thielemann, F.-K., Nomoto, K., & Hashimoto, M. 1996, ApJ, 460, 408
Timmes, F. X., Woosley, S. E., & Weaver, T. A. 1995, ApJS, 98, 617
Tozzi, P., Rosati, P., Ettori, S., Borgani, S., Mainieri, V., & Norman, C. 2003, ApJ, 593, 705
Tsai, J. C. 1994a, ApJ, 423, 143
——. 1994b, ApJ, 429, 119
Umeda, H., & Nomoto, K. 2003, Nature, 422, 871
van Dokkum, P. G., Franx, M., Kelson, D. D., & Illingworth, G. D. 1998, ApJ, 504, L17
Weisskopf, M. C., Brinkman, B., Canizares, C., Garmire, G., Murray, S., & Van Speybroeck, L. P. 2002, PASP, 114, 1
White, D. A. 2000, MNRAS, 312, 663
White, D. A., Fabian, A. C., Johnstone, R. M., Mushotzky, R. F., & Arnaud, K. A. 1991, MNRAS, 312, 663
White, S. D. M., Navarro, J. F., Evrard, A. E., & Frenk, C. S. 1993, Nature, 366, 429
Woosley, S. E., & Weaver, T. A. 1995, ApJS, 101, 181
Wyithe, S., & Loeb, A. 2003, ApJ, 588, L69
Xu, H., et al. 2002, ApJ, 579, 600
Xu, H., Ezawa, H., Fukazawa, Y., Kikuchi, K., Makishima, K., Ohashi, T., & Tamura, T. 1997, PASJ, 49, 9